Appl. Phys. B 70, 645–647 (2000) / Digital Object Identifier (DOI) 10.1007/s003400000264

Applied Physics B
Lasers
and Optics

Rapid communication

Seeded and spontaneous light hexagons in $LiNbO_3$:Fe

S. Odoulov[1], **B. Sturman**[2], **E. Krätzig**[3]

[1] Institute of Physics, National Academy of Sciences, 252 650 Kiev, Ukraine
[2] Institute of Automation and Electrometry of RAN, 630 090 Novosibirsk, Russia
[3] Fachbereich Physik, Universität Osnabrück, Osnabrück, 49080 Germany

Received: 9 February 2000/Published online: 8 March 2000 – © Springer-Verlag 2000

Abstract. The first observation of optical hexagons in a medium with dominating photovoltaic charge transport – in $LiNbO_3$:Fe – is reported. The optimum conditions for hexagon observation are revealed and discussed. The dynamics of hexagon formation are also studied.

PACS: 42.65.Sf; 42.70.Mp; 42.40.Pa

Spatial pattern formation in nonequilibrium systems has been the subject of detailed studies in fluid mechanics, solid state physics, chemistry, biology, and, recently, also in nonlinear optics (see, e.g., a comprehensive review [1]). A system with an initially homogeneous spatial distribution of a certain parameter (e.g., the transverse intensity distribution in a light beam) undergoes a transition to a regular spatial pattern (e.g., with a one-dimensional or a two-dimensional periodic transverse variation of the light intensity) at a certain critical value of the control parameter (e.g., coupling strength for nonlinear wave mixing). A typical example is the spontaneous appearance of hexagonal structures in photorefractive crystals with two counterpropagating pump waves of the same frequency, first observed by Honda in $KNbO_3$ [2]. This paper [2] inspired further experiments that resulted in the observation of optical hexagons also in $BaTiO_3$ and doped $KNbO_3$ (see [3, 4] and references therein).

In nearly all these experiments the interaction geometry was chosen in such a way that the hexagon side lobes were coupled only to the counterpropagating pump wave, i.e., reflection photorefractive gratings were dominant [5]. The space-charge formation occurred because of diffusion of photoexcited carriers, i.e., $\pi/2$-shifted index gratings were recorded. The theory [6–10] shows the possibility for pattern formation also for photorefractive crystals with local response (i.e., with π-shifted or 0-shifted reflection photorefractive gratings), but no particular final light pattern can be predicted.

This contribution reports on the first experimental observation and study of hexagonal pattern formation in $LiNbO_3$:Fe with a dominating photovoltaic charge transport [11], i.e., with a mixed nonlinear response that is closer to a local than to a nonlocal response (grating phase shift between $\pi/2$ and π, closer to π). We study the influence of a seeding beam and the dynamics of hexagon formation.

1 Spatial structures and conditions of observation

The experimental setup is sketched in Fig. 1. A pump beam of a single transverse mode Ar^+ laser is focused onto the sample by a high-quality lens L1 of 40-cm focal length. With a 20-mW pump beam in front of lens L1 the estimated light intensity in the sample is $\approx 100\,W/cm^2$. The backward pump beam, necessary for pattern formation, arises because of reflection from the crystal's rear face (reflectivity $\approx 16\%$). The polar axis of the sample is aligned in such a way that the reflected beam is amplified because of two-beam coupling.

An auxiliary light beam of variable power (up to 100 mW) is incident onto the same area of the crystal and serves as background illumination. This beam is loosely focused onto the sample to ensure a photoconductivity comparable to that originating from the pump beam.

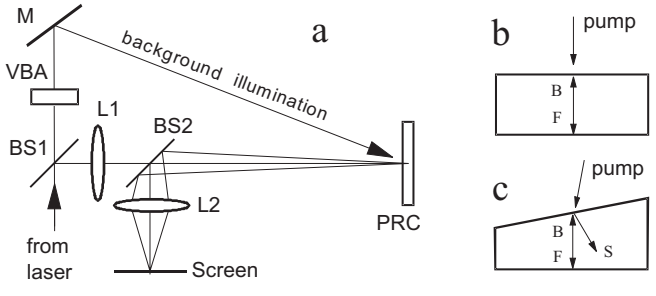

Fig. 1. a Schematic drawing of the experimental setup. BS1,2 are beamsplitters, L1,2 are lenses, PRC is a photorefractive $BaTiO_3$ crystal and VBA is a variable beam attenuator. **b**, **c** Propagation direction of the forward (F) and the backward (B) pump wave (reflected from the rear side) inside the sample. Note the appearance of the seeding wave (S) for the sample with imperfectly parallel faces (**c**)

Three z-cut samples doped with 0.02 wt. % of Fe (labelled further as 1, 2, and 3) are used. The thicknesses l and the angles α between the front and the rear faces of the samples are 5.5 mm and $\leq 0.06°$, 4.3 mm and 0.8°, 2.0 mm and 1.7°, respectively. The effective photovoltaic field for the samples used is $E_{\rm ph} \approx 35\,{\rm kV/cm}$ [12], i.e., it is considerably larger than the diffusion field $E_{\rm D} \approx 15\,{\rm kV/cm}$.

With the help of lens L2, either the far-field or the near-field intensity distribution is projected onto the screen. The developing patterns could be monitored with a VCR camera; in some experiments a detector was placed instead of the screen to measure the scattering intensity.

For sample 1, the spatial distribution of light scattered into the backward direction is usually irregular with a pronounced speckle structure. However, for this sample we occasionally observed hexagon structures like that shown in Fig. 2a during the initial stage of illumination. For 300 recording cycles such transient hexagons appeared only three times. Their angular size was about 1.2° in air. For sufficiently long exposure the light distribution always looked irregular with a larger angular divergence (Fig. 2b).

Well reproducible stable hexagons are observed with samples 2 and 3 possessing imperfectly parallel input and output faces (Fig. 3). The samples are aligned in such a way that the wave B reflected from the rear face is exactly counterpropagating with respect to the forward pump wave F. The part of the wave B reflected into the sample from the input face serves as a seeding beam S (Fig. 1c).

We have found that hexagons can be seeded efficiently even in directions which are far from the natural directions of the hexagon side lobes. For sample 2, the position of the seeding beam in the far-field pattern coincides with the position of one of the side lobes (see Fig. 3a). In other words, we have

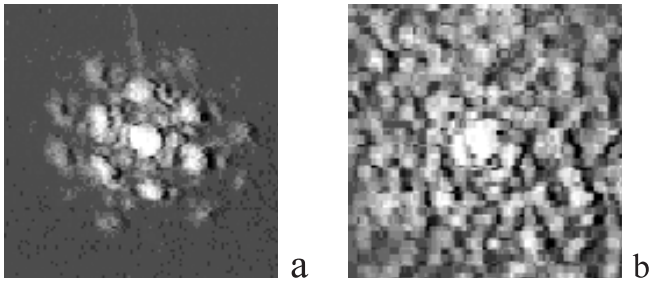

Fig. 2a,b. Far-field intensity distribution for sample 1 at 80 s (**a**) and 300 s (**b**) after beginning of exposure

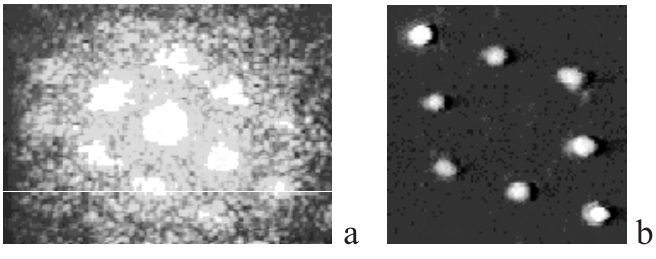

Fig. 3a,b. Steady-state far-field intensity distribution for sample 2 (**a**) and sample 3 (**b**). The seeding beam coincides with the hexagon upper left spot for (**a**) and is in the upper left corner of the frame (**b**). The central spot is filtered out in **b**

here $k_{\perp s} \equiv k_{\perp 1}$, where $k_{\perp s}$, $k_{\perp 1}$ are the transverse components of the wave vectors for the seed (s) and the hexagon beam (1). For sample 3, we have another relation, $k_{\perp s} = k_{\perp 1} + k_{\perp 2}$, where $k_{\perp 1,2}$ are the transverse wave vectors of two adjacent side lobes (see also Fig. 3b). This direction of the seeding beam coincides with the so-called harmonic $\sqrt{3}$ of the principal hexagon [13].

The size and orientation of the seeded hexagons are insensitive to the light wavelength within the studied spectral interval 476–514 nm. The polarization of the side beams is the same as that of the pump beams. No frequency detuning is detected for the hexagon side lobes: The observed near field pattern is stable in time at least during half a minute, proving that frequency shift (if any exists) is not more than 0.01 Hz.

With (the thinnest) sample 3, hexagons were generated also with a feedback mirror ensuring the backward pump beam.

Let us discuss these results before we describe the temporal evolution of hexagon intensity. For the first time to our knowledge, hexagon excitation is achieved in a medium with a dominating local (photovoltaic) contribution to the photorefractive response. The coupling strength related to the photovoltaic charge transport in sample 3 is $\gamma l \approx 5.0$. It is higher than the threshold values $\gamma l_{\rm th} \approx 3.5 - 4.5$ estimated for local response on the basis of the available theoretical models [8, 9]. Note that the evaluated coupling strength, which is only due to diffusion, is $\gamma l \approx 2.2$ for this sample, considerably smaller than the theoretical threshold $\gamma l_{\rm th} = 3.6$ for diffusion transport [8]. While these estimates show the prime importance of local response, they cannot exclude some influence of diffusion charge transport on the pattern formation via energy exchange between the pump waves.

The second important result is that excitation of hexagons becomes easier in moderately thin samples. In spite of the fact that the coupling strength for the thick sample 1 is much higher than the threshold of pattern formation, the hexagons appear only in about each hundredth recording cycle and they are not stable in time. We would like to emphasize that this poor reproducibility of hexagons for sample 1 could be an indication that the hexagons become unstable at excessively large coupling strengths. The transition from hexagons to irregular structures with increasing nonlinear coupling has been predicted in computer simulations for a Kerr medium with a feedback mirror [14]. The interesting question whether the observed irregular patterns exhibit deterministic spatial chaos [15] is beyond the scope of this paper.

The third result is that the presence of an oblique coherent light beam (serving as a seed) apart from the two counterpropagaing pump beams can facilitate hexagon formation. A similar effect is known from experiments with sodium vapor [16]. The distinctive feature of our case is the possibility to excite a hexagon via higher harmonics.

2 Hexagon dynamics

We now turn to the description of the dynamics of hexagon formation. Figure 4a,b shows typical time dependencies of the total intensity of light scattered into the ring covering the hexagon spots for sample 3 with a feedback ensured by reflection from the rear face and from an auxiliary high-reflective mirror, respectively.

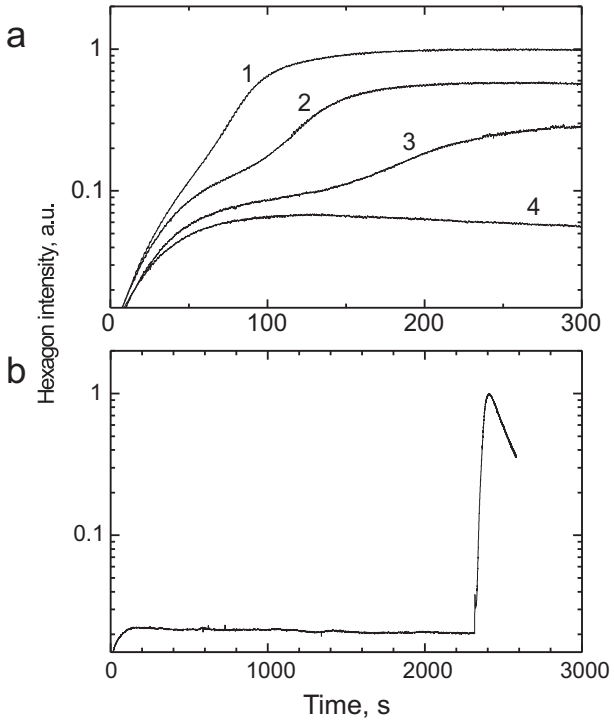

Fig. 4a,b. Dynamics of hexagon development for sample 3 at 0.488 μm with (**a**) and without (**b**) a seeding beam. The coupling strength in **a** is gradually decreasing from trace 1 to trace 4 because of growing intensity of the background illumination

Traces 1–4 in Fig. 4a correspond to increasing intensity of the background illumination, i.e., decreasing strength of the nonlinearity. A limited coherence length of the laser (no etalon inside the cavity) prevented here any grating recording involving interference of the auxiliary and the pump (or side) beams. Note an obvious acceleration of the intensity growth in the intermediate stage for each of the traces except trace 4. This acceleration corresponds to the emergence of the hexagon. The coupling strength for trace 4 is below the threshold and the hexagon does not appear. The closer the coupling strength is to its threshold value, the longer the hexagon build-up time becomes (time interval between the start of illumination and the acceleration of intensity growth). The longest time we measured is about one hour. This indicates that the pattern formation in $LiNbO_3$ is a critical phenomenon with a typical slowing down effect near the threshold [17].

To describe hexagon temporal dynamics, the interaction of several weak side lobes has to be taken into account. A suitable theory for hexagons in a medium with local or mixed local/nonlocal response is not yet available. However, our experimental results allow for some qualitative conclusions, as is explained below.

The standard scenario for the onset of a hexagon is via a subcritical bifurcation [1], i.e., the hexagon appears at the threshold with a certain finite intensity (hard mode of excitation), and optical bistability [18, 19] can be observed in the vicinity of the threshold. For hexagons in $BaTiO_3$ (dominating nonlocal response), this was predicted [13] and recently proved experimentally [20].

The dynamics of hexagon development in $LiNbO_3$:Fe with a feedback mirror is qualitatively similar to that in $BaTiO_3$. In particular, a step-like onset of the oscillation (hard excitation) is observed (Fig. 4b), pointing to subcritical behavior and a similarity to a first order phase transition [20]. At the same time, for seeded hexagons the onset of oscillation is smooth (Fig. 4a), with the intensity increasing gradually from the noise level to the steady state value. This behavior suggests a supercritical bifurcation and a similarity to a second order phase transition [1]. The presence of the seed beam does not reduce the hexagon excitation to a thresholdless convective instability, but it changes the type of bifurcation.

Acknowledgements. Partial financial support from the Deutsche Forschungsgemeinschaft (SFB 225, D9) and the Civilian Research and Development Foundation (UP2-322) is gratefully acknowledged.

References

1. M.C. Cross, P.C. Hohenberg: Rev. Mod. Phys. **65**, 854 (1993)
2. T. Honda: Opt. Lett. **18**, 598 (1993)
3. A.V. Mamaev, M. Saffman: Opt. Lett. **22**, 283 (1997)
4. C. Denz, M. Schwab, M. Sedlatschek, T. Tschudi, T. Honda: J. Opt. Soc. Am. B **15**, 2057 (1998)
5. A.V. Mamaev, M. Saffman: Recent reports of hexagons related to transmission grating recording, Europhys. Lett. **34**, 669 (1996)
6. M. Saffman, A.A. Zozulya, D.Z. Anderson: J. Opt. Soc. Am. B **12**, 1409 (1994)
7. B. Sturman, A. Chernykh: J. Opt. Soc. Am. B **12**, 1384 (1995)
8. T. Honda, P. Banerjee: Opt. Lett. **21**, 779 (1996)
9. A. Chernykh, B. Sturman, M. Aguilar, F. Agullo-Lopez: J. Opt. Soc. Am. B, **14**, 1754 (1997)
10. O. Sandfuchs, F. Kaiser, M.R. Belic: J. Opt. Soc. Am. B **15**, 2070 (1998)
11. B. Sturman, V. Fridkin: *The photovoltaic and photorefractive effects in noncentrosymmetric materials* (Gordon and Breach, Philadelphia 1992)
12. E. Krätzig, H. Kurz: J. Electrochem. Soc. **124**, 131 (1977)
13. P.M. Lushnikov: JETP **86**, 614 (1999)
14. D. G. D'Allessandro, W.J. Firth: Phys. Rev. Lett. **66**, 2597 (1991)
15. R. Blumrich, T. Kobialka, T. Tschudi: J. Opt. Soc. Am. B **12**, 1384 (1995)
16. J. Pender, L. Hesselink: J. Opt. Soc. Am. B **7**, 1361 (1990)
17. D. Engin, S. Orlov, M. Segev, G.C. Valley, A. Yariv: Phys. Rev. Lett. **74** 1743 (1995)
18. A. Petrossian, M. Pinard, A. Maitre, J.-Y. Courtois, G. Grynberg: Europhys.Lett. **18**, 689 (1992)
19. T. Ackemann, B. Giese, B. Schaepers, W. Lange: J. Opt. B **1**, 70 (1999)
20. S. Odoulov, M. Goul'kov, O. Shinkarenko: Phys. Rev. Lett. **83**, 3637 (1999)